Short-range-order effects in Cu_xPt_{1-x}

J. Banhart
Institut für Physikalische Chemie, Universität München, D-8000 München 2, Federal Republic of Germany

P. Weinberger
Institut für Technische Elektrochemie, Technische Universität Wien, A-1060 Wien, Austria

J. Voitländer
Institut für Physikalische Chemie, Universität München, D-8000 München 2, Federal Republic of Germany
(Received 22 September 1988; revised manuscript received 28 March 1989)

The effects of short-range order on the electronic structure of Cu_xPt_{1-x} are investigated using the fully relativistic Korringa-Kohn-Rostoker embedded-cluster method (KKR-ECM). It is found that, with increasing distance to the origin, effects of short-range order become less and less important. By performing configurational averages it is shown that the (single-site) KKR-coherent-potential approximation (KKR-CPA) is indeed an excellent approximation to describe the electronic structure of substitutionally disordered alloys. The results also show an interesting behavior of the density of states at the Fermi energy with respect to the short-range-order parameters for the first and second shell α_1 and α_2.

I. INTRODUCTION

It is well known that the single-site coherent-potential approximation (CPA) does not account for short-range-order effects. In order to study such effects, one of the most promising approaches is the so-called embedded-cluster method (ECM). In this method one treats a cluster of atoms embedded in an effective medium determined, e.g., by means of the CPA. The ECM is not a self-consistent theory like the CPA. It was originally applied in connection with tight-binding Hamiltonians[1,2] and then generalized to the more realistic muffin-tin Hamiltonians.[3,4] Within the ECM the off-site diagonal Green's functions are calculated directly by means of Brillouin-zone integrals, i.e., by means of an approach treating the embedding problem rigorously. By using a multiple-scattering approach for both the single-site CPA and the ECM, namely the Korringa-Kohn-Rostoker (KKR) method, a discussion of short-range-order effects can be based on the same numerical footing as the single-site KKR-CPA.

Since one of the components in Cu_xPt_{1-x} is a $5d$-electron metal, undoubtedly relativistic effects are of crucial importance for spectral densities. For this reason the fully relativistic version of the KKR-CPA (Ref. 5) and of the KKR-ECM (Ref. 6) has to be applied. This not only implies that the computational effort is substantially increased as compared to the nonrelativistic KKR-CPA (Ref. 7), and the nonrelativistic KKR-ECM (Refs. 3 and 4), but also that the group-theoretical means have to be more sophisticated.[6,8]

Short-range order is important for all physical observables depending on the local environment. Such a quantity is, for example, the nuclear spin-lattice relaxation rate, which has been studied for different environments of Pt atoms in Cu_xPt_{1-x} in a previous paper[9] using the relativistic KKR-ECM. Such a study is yet comparatively easy to perform, since only (environment-dependent) partial local densities of states at the Fermi energy are needed.[9,10] In the present paper the energy regime of the whole valence region is investigated by considering up to two shells of neighbors. The second shell is important, since it was argued that in $Cu_{50}Pt_{50}$ short-range ordering "starts" beyond the first shells of neighbors.[9]

Using the values of environment-dependent densities of states at the Fermi energy we extend our study up to four shells of neighbors. Furthermore, we show that at least for the present system the single-site KKR-CPA is indeed an excellent approximation to describe the electronic structure of substitutionally disordered alloys.

II. COMPUTATIONAL DETAILS

The calculations were performed in three major steps. The first step was to solve the relativistic KKR-CPA equations self-consistently. The alloy potentials used were non-self-consistent and correspond to full Slater exchange. For Cu_xPt_{1-x} this potential setup has proved to give excellent agreement of theoretically calculated nuclear spin-lattice relaxation rates[9] and electrical resistivities[11] with corresponding experimental values. Probably effects of charge transfer are rather small in Cu-Pt so that our non-self-consistent potential would not differ too much from a self-consistent one. Nevertheless, a self-consistent calculation of the site potentials—which within the relativistic KKR-CPA at the present stage of our work is not yet feasible in a routine manner—is desirable in order to eliminate ambiguities due to the potential construction. For both the KKR-CPA and the KKR-ECM all Brillouin-zone integrals are calculated using the 21 special directions of Fehlner and Vosko.[12] It should be mentioned that all calculations were performed

along the real axis.

The second step was the calculation of the off-site diagonal scattering path operators $\tau^{ij}(\varepsilon)$, where $i \neq j$, by means of Brillouin-zone integrations using the single-site KKR-CPA scattering amplitudes. The number of scattering path operators which has to be calculated can be held rather low if one recognizes that they belong to a small number of equivalence classes, the members of which can be transformed into each other by similarity transformations. Thus only a total of four (6,12,14) of such operators has to be calculated if a total of one (2,3,4) shell of neighbors is included. If one chooses a fixed-point mesh for the line integrals along the special directions, one can calculate the integrals for all inequivalent scattering path operators simultaneously and therefore has to calculate the inverse KKR matrix only once for each $\mathbf{k}$ point, thus saving a lot of computing time. We used a 200-point Gaussian formula for the line integrals. This numerical technique allows us to integrate a polynomial of degree 399 exactly. The functions we integrate, the components of the CPA scattering path operator, are a collection of peaks broadened by disorder and can therefore be approximated by such a polynomial with sufficient accuracy. In order to check this integration procedure we calculated line integrals using Gaussian formulas with 20, 50, and 100 points. We found that in all cases the results were stable for already 100 points.

The third step was the calculation of site diagonal scattering path operaors at the origin of clusters of atoms with a specified atomic configuration embedded in the CPA medium. From these operators cluster densities of states or other properties can be calculated. It is important to note that not all possible cluster configurations (2^N in an N-atom cluster) have to be treated separately, but only those which are nonequivalent in the sense that they cannot be transformed into each other by spatial rotations. By considering, for example, only a first shell of neighbors, there is a total of 144 inequivalent configurations per specified atom at the origin in an fcc lattice. The size of the cluster matrix in this case is 234. For a cluster including also the second shell of neighbors, the corresponding size of the cluster matrix is already 342 with an exploding total number of configurations. Taking, for example, the fourth shell of neighbors into account as applied in the following for one particular case, the size of the matrix increases to 990. Since the cluster matrices are energy dependent, the computational effort very quickly becomes prohibitive with an increasing number of shells.

In the following, the term "CPA atom" means that at a particular site in the embedded cluster, the effective t matrix as determined by the KKR-CPA is used as single-site t matrix. If all sites except the origin are occupied by "CPA atoms," the KKR-ECM densities of states reduce exactly to the densities of states as defined within the KKR-CPA.

The calculated cluster operators $\tau_J^{00}(\varepsilon)$ and related cluster electronic properties X_J refer to a definite microscopic cluster configuration J. In order to obtain a macroscopic observable, a configurational average has to be performed including all possible cluster configurations and their statistical weights. The macroscopic state of order may be described using short-range-order parameters:

$$\alpha_r^{AB} = 1 - \frac{P_r^{AB}}{c_B} \ . \tag{1}$$

In (1) an A atom is at the center of the rth shell, c_B denotes the macroscopic concentration of species B, and P_r^{AB} is the pair probability of finding a B atom anywhere in the rth shell around an A atom. Since $\alpha_r^{AB} = \alpha_r^{BA} = \alpha_r$ and $0 \leq P_r \leq 1$, the range of α_r is given by

$$1 - \frac{1}{\max\{c_A, c_B\}} \leq \alpha_r \leq 1 \ . \tag{2}$$

For a configurational average it is assumed that the statistical weight of a given configuration depends only on the number of A/B atoms, n_A/n_B, in the shell considered. This implied that the situation is described by pair probabilities only. The weight for an A-centered configuration with n_B B atoms in the rth shell $J_r(A, n_B, n)$, $n_A + n_B = n$, is given by

$$P^{J_r(A,n_B,n)} = (P_r^{AB})^{n_B}(1 - P_r^{AB})^{n-n_B} \ . \tag{3}$$

The configurational average of X_J is then defined as

$$\begin{aligned} \langle X \rangle_r^A &= \sum_{J=J_r(A)} P^J X_J \\ &= \sum_{n_B=0}^{n} \left\{ [c_B(1-\alpha)]^{n_B} [1 - c_B(1-\alpha_r)]^{n-n_B} \right. \\ &\qquad \left. \times \sum_{J=J(A,n_B)} X_J \right\} , \end{aligned} \tag{4}$$

and analogous for $\langle X \rangle_r^B$.

III. RESULTS

The present results can be grouped into three sets of figures. In group I the Cu (Pt) density of states (DOS) and its Pt $d^{3/2}$- and Pt $d^{5/2}$-like contributions corresponding to a Cu (Pt) atom at the origin and 12 first neighbors of either only Cu or only Pt is compared for three different alloys of Cu_xPt_{1-x}, namely $x = 0.15$, 0.50, and 0.71, with the corresponding results of a KKR-CPA calculation (Figs. 1 and 2).

Group II concentrates on a single alloy, namely $Cu_{50}Pt_{50}$ (Figs. 3–5). Here the Cu- (Pt-) like DOS and its $d^{3/2}$- and $d^{5/2}$-like contributions for a Cu (Pt) atom in the origin and (a) a first and second shell of neighors of either only Cu or only Pt and (b) a first-neighbor shell of CPA atoms and a second-neighbor shell of either only Cu or only Pt is shown in relation to the corresponding KKR-CPA results. Also considered is the case when for a Cu (Pt) atom at the origin the first and second shell of neighbors is occupied by Cu and Pt atoms according to the ordered CuPt superstructure ($L1_1$).

Group III finally deals with the DOS at the Fermi energy as calculated, for example, as a function of the short-range-order parameters α_1 and α_2 or in relation to the single-site KKR-CPA (Figs. 6–8).

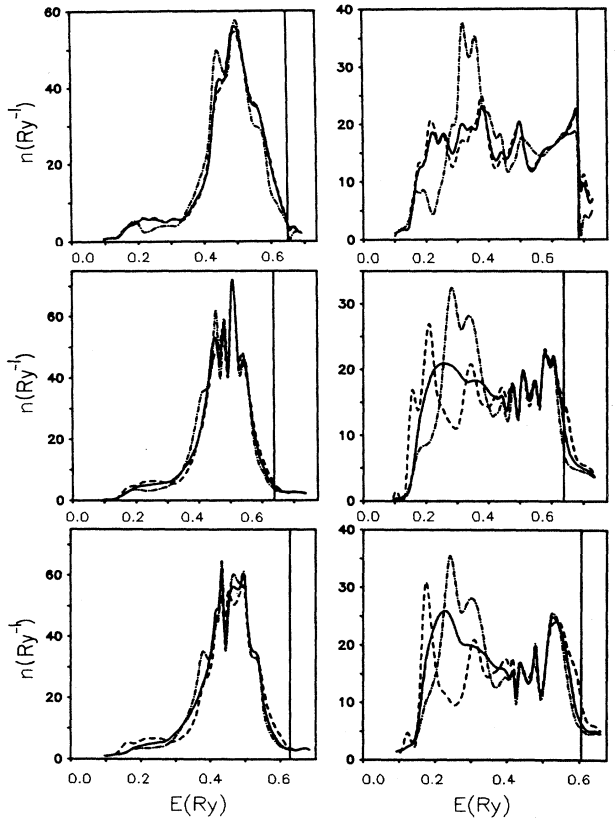

FIG. 1. Cu-like (left panel) and Pt-like (right panel) DOS for $Cu_{15}Pt_{85}$, $Cu_{50}Pt_{50}$, and $Cu_{71}Pt_{29}$ (from top to bottom). In each entry the solid line corresponds to the single-site KKR-CPA calculation, the dashed line to 12 Pt first neighbors, and the dashed-dotted line to 12 Cu first neighbors. Vertical line: Fermi energy.

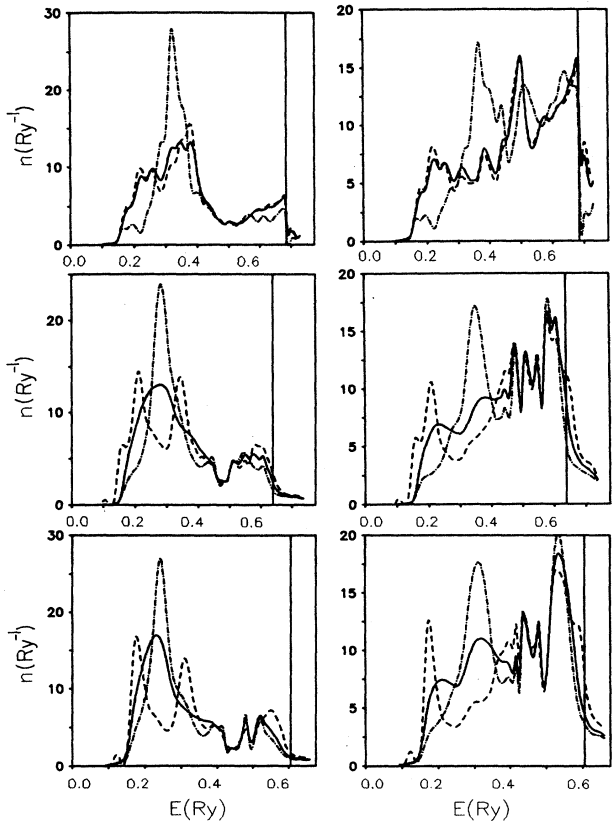

FIG. 2. Pt $d^{3/2}$-like (left panel) and Pt $d^{5/2}$-like (right panel) DOS for $Cu_{15}Pt_{85}$, $Cu_{50}Pt_{50}$, and $Cu_{71}Pt_{28}$ (from top to bottom). In each entry the solid line corresponds to the single-site KKR-CPA calculation, the dashed line to 12 Pt first neighbors, and the dashed-dotted line to 12 Cu first neighbors. Vertical line: Fermi energy.

A. First-neighbor-shell effects

It is perhaps surprising to find out from Fig. 1 that the Cu-like DOS is little influenced by the occupation of the first shell of neighbors, whereas the Pt-like DOS obviously is rather sensitive to it. This strong dependence of the Pt DOS on the environment, however, is more or less restricted to an energy regime below about 0.4 Ry and to the vicinity of the Fermi energy. It is interesting to see the Pt DOS of Fig. 1 resolved into $d^{3/2}$- and $d^{5/2}$-like contributions. In Fig. 2 (left panel), for Cu only nearest neighbors, the peak in the $d^{3/2}$- like Pt DOS moving from about 0.32 to 0.24 Ry with respect to increasing Cu concentration, is separated from the corresponding $d^{5/2}$-like peak (see right panel) by about 0.06 Ry, which is about half of the spin-orbit splitting for Pt. For Pt only first neighbors, one can see from Fig. 2 the building up of two $d^{3/2}$-like peaks and one $d^{5/2}$-like peak. The DOS of a Pt atom surrounded by 12 Cu atoms is very much like that of a Pt impurity in a Cu host with virtual bound states in the corresponding energy regimes, whereas a Pt neighborhood tends to produce a peak structure closer to that in pure Pt.

It is interesting to note how the single-site KKR-CPA reflects the two "extreme configurations" of either only Cu or only Pt first neighbors. In particular from the $d^{5/2}$-like Pt DOS one can see that (for energies below 0.4 Ry) the single-site KKR-CPA result indeed has round peaks in the vicinity of the peaks generated by either only

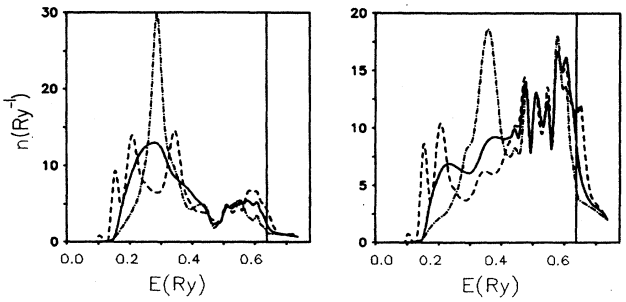

FIG. 3. Pt $d^{3/2}$-like (left panel) and Pt $d^{5/2}$-like (right panel) DOS in $Cu_{50}Pt_{50}$. In each entry the solid line corresponds to the single-site KKR-CPA calculation, the dashed line to a cluster with the first and second shell of neighbors occupied by Pt atoms only, and the dashed-dotted line to the same cluster, but occupied by Cu atoms only. Vertical line: Fermi energy.

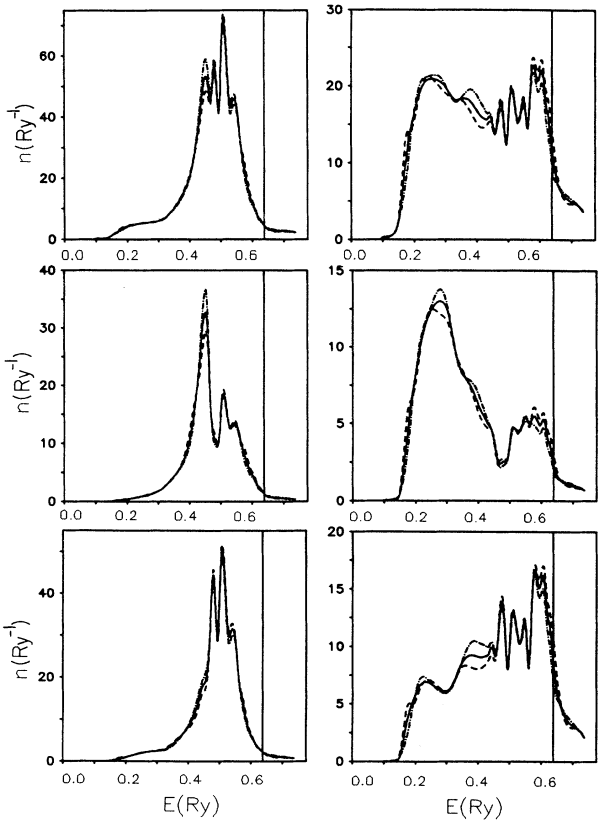

FIG. 4. Componentlike DOS and its $d^{3/2}$- and $d^{5/2}$-like contributions (from top to bottom) for a Cu atom (left panel) and a Pt atom (right panel) at the origin in $Cu_{50}Pt_{50}$. In each entry the solid line corresponds to the single-site KKR-CPA calculation, the dashed line to a cluster with a first shell of CPA atoms and a second shell of neighbors occupied by Pt atoms only, and the dashed-dotted line to the same cluster, the second shell occupied by Cu atoms only. Vertical line: Fermi energy.

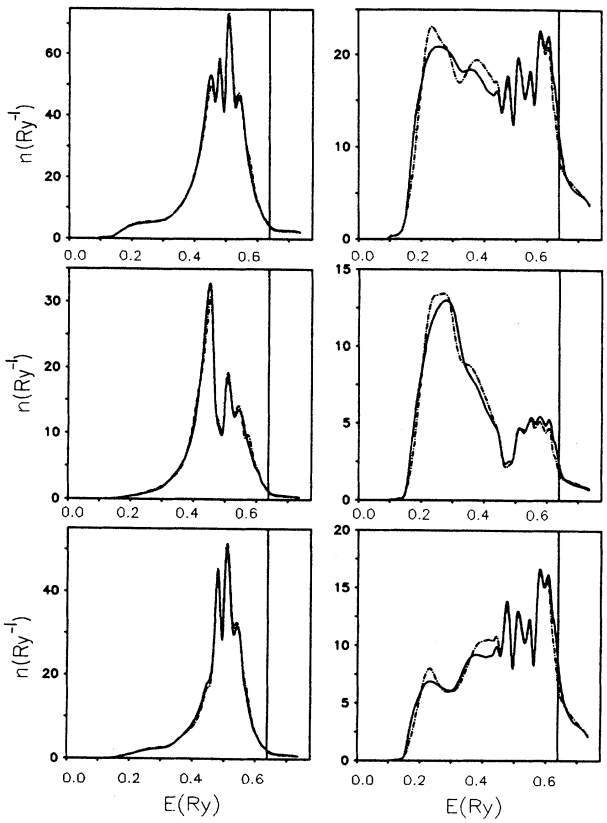

FIG. 5. Componentlike DOS and its $d^{3/2}$- and $d^{5/2}$-like contributions (from top to bottom) for a Cu atom (left panel) and a Pt atom (right panel) at the origin in $Cu_{50}Pt_{50}$. The solid line corresponds to the single-site KKR-CPA results, the dashed line to an occupation of the first and the second shell of neighbors according to the ordered superstructure $L1_1$. Vertical line: Fermi energy.

Cu or only Pt first neighbors. These are the peaks to be correlated with "chemical bonding" between the alloy constituents. In the $d^{3/2}$-like Pt DOS the CPA-DOS even reduces to a single peak lying between the two peaks of the Pt-rich neighborhood.

B. Second-neighbor-shell effects

Comparing Fig. 3 with the entries for $Cu_{50}Pt_{50}$ in Fig. 2, it is evident that by including a second shell of neighbors of either only Cu or only Pt atoms, the changes are rather small even for a Pt atom at the origin. For a Pt atom surrounded by a Cu neighborhood, the main influence of the second shell is that the peaks become higher and narrower, i.e., more impuritylike than the corresponding peaks in Fig. 2. For a Pt neighborhood it appears that where the Pt $d^{3/2}$- and Pt $d^{5/2}$-like DOS for $Cu_{50}Pt_{50}$ have shoulders at about 0.15 Ry, there are now in Fig. 3 well developed peaks and the whole structure is broader. All the other features are more or less unchanged.

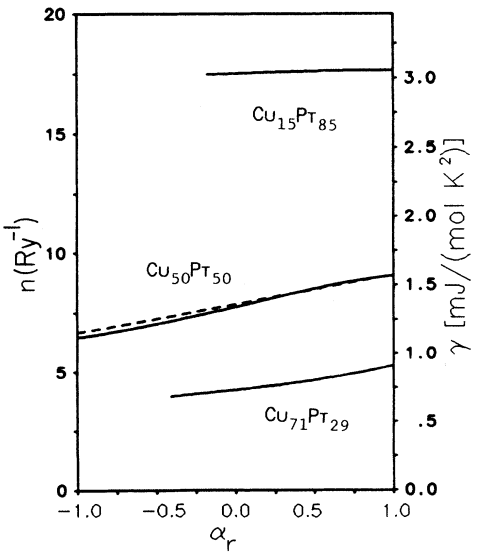

FIG. 6. Configurationlly averaged DOS at the Fermi energy as function of the short-range parameter α_1 (solid line) and α_2 (dashed line). The scale on the right side refers to the units of the linear coefficient of the specific heat.

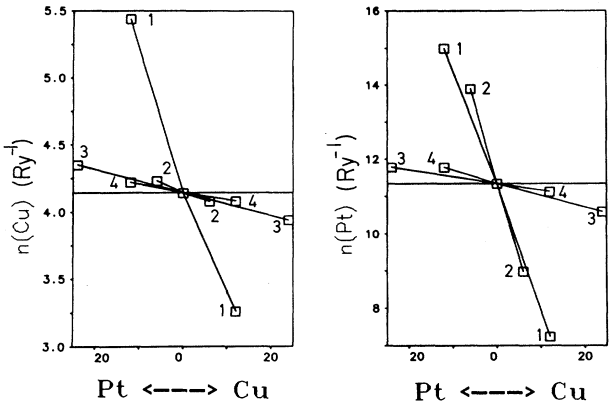

FIG. 7. Density of states at the Fermi energy for clusters (indicated by the numbers) occupied by only Cu or Pt and the other sites occupied by CPA atoms. Left: Cu at the origin, right: Pt at the origin. Abscissa: number of sites in a particular shell; arrows indicate if the shell is occupied by Cu or Pt. (1) First shell either only Cu or only Pt, (2) first shell CPA atoms, second shell either only Cu or only Pt, (3) first and second shell CPA atoms, third shell either only Cu or only Pt, and (4) first-, second-, and third-shell CPA atoms, fourth shell either only Cu or only Pt. The horizontal line refers to the single-site KKR-CPA result.

In order to estimate separately the effect of a second shell of specified neighbors, Fig. 4 shows the case that the first shell of neighbors is occupied by CPA atoms and the second shell by either only Cu or only Pt atoms. Now both kinds of atoms at the origin are quite insensitive to the occupation in the second shell, with the biggest effects occurring in the Pt $d^{5/2}$-like DOS. It is therefore not at all surprising that the single-site KKR-CPA covers both cases of extreme occupation of the second shell of neighbors very well.

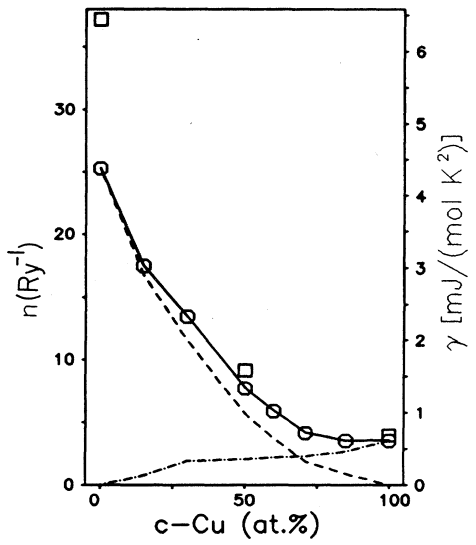

FIG. 8. Single-site KKR-CPA densities of states at the Fermi energy as decomposed with respect to the components Cu and Pt and compared with corresponding experimental linear coefficients of the specific heat (squares). The theoretical values for the pure metals are from Refs. 17 and 18, the experimental values (squares) from Refs. 19 and 20.

It is well known that the CPA represents a configurational average. By using second-shell clusters, however, it is possible to illustrate how much the single-site KKR-CPA resembles "locally" the ordered CuPt superstructure. In this type of ordered structure the first, third, fifth, etc. shell around a central Pt atom is occupied by 50% Cu and 50% Pt atoms, while the second shell is entirely occupied by Cu atoms, the fourth shell by Pt, and so on. In Fig. 5 the single-site KKR-CPA results are compared with the case that the occupation of the first and second shell of neighbors is in accordance with the $L1_1$ (ordered) superstructure. This comparison is amazing, since for a Cu atom at the origin the differences between the "statistically disordered" and the "ordered" case are indeed marginal and even for a Pt atom at the origin the single-site KKR-CPA gives a fairly accurate description for the electronic structure of the "ordered" cluster embedded in the CPA medium. Figure 5 has to be regarded as a convincing illustration for the frequently used statement that the disordered state is a suitable reference medium for perturbation expansions of physical properties of ordered phases in terms of order parameters. Such expansions are, for example, used in the generalized perturbation method (GPM).[14–16]

C. Short-range-order effects at the Fermi energy

Considering all nonequivalent configurations of the first shell, by means of Eq. (4) the configurational average has been calculated for a number of values of the SRO parameter α_1. In Fig. 6 the configurationally averaged DOS at the Fermi energy is shown as a function of α_1. This figure actually shows that although the Pt site at the origin is rather sensitive to local arrangements, at the Fermi energy these effects are much less drastic. For $Cu_{50}Pt_{50}$, for example, the configurationally averaged density of states changes from 6.6 states/Ry for $\alpha_1=-1$ (complete order) to about 9 states/Ry for $\alpha_1=1$ (complete segregation). Apparently with respect to α_1, short-range ordering reduces the linear coefficient of the specific heat. A similar behavior can be seen with respect to α_2. Because of the restricted range of pair probabilities [see Eq. (1)] these changes are less important for Cu- or Pt-rich alloys. Note that in Fig. 6 the scale on the right-hand side refers to units facilitating a comparison of the bare DOS to the linear coefficient of the specific heat.

In terms of the DOS at the Fermi energy in Fig. 7 the question is addressed of how far out from a particular site short-range-order effects matter. For this purpose, embedded clusters with a Cu or Pt atom at the origin and with either only Cu or only Pt occupation in a particular shell are considered, while all other sites are occupied by CPA atoms. These "shell-dependent" DOS's are plotted versus the number of sites in the corresponding specified shell and compared to the values of the single-site KKR-CPA. The slopes of the lines connecting the values of the

TABLE I. $[\tau^{ECM}(E_F)-\tau^{CPA}(E_F)]/\tau^{CPA}(E_F)$.

Irreducible component	$Cu_{15}Pt_{85}$		$Cu_{50}Pt_{50}$		$Cu_{71}Pt_{29}$	
	Re	Im	Re	Im	Re	Im
$\Gamma_6^+(s^{1/2})$	−0.000 07	−0.000 95	−0.000 04	−0.000 89	−0.000 06	0.000 22
$\Gamma_6^-(p^{1/2})$	0.000 02	0.012 24	0.000 13	0.011 92	0.000 40	0.009 55
$\Gamma_8^-(p^{3/2})$	−0.000 40	−0.000 69	−0.001 69	−0.001 28	−0.004 22	0.003 76
$\Gamma_7^+(d^{5/2})$	−0.009 80	0.004 61	0.005 20	0.018 78	−0.000 49	−0.003 98
$\Gamma_8^+(d^{3/2})$	−0.001 00	0.004 21	0.003 29	0.008 59	−0.000 99	−0.000 06
$\Gamma_8^+(d^{5/2})$	−0.004 21	0.001 10	−0.000 27	0.005 08	−0.002 39	−0.004 68
$\Gamma_8^+(d^{3/2,5/2})$	0.011 69	0.008 05	0.208 20	0.029 68	−0.199 40	0.004 57

shell DOS with the CPA values express the influence *per atom* of the specified shell on the DOS of the central site. As one can see from Fig. 7 for the Cu-like DOS only effects from the first shell are of some importance, whereas for the Pt-like DOS effects beyond the second shell are of minor importance. It should be noted that by filling up the shells successively with CPA atoms explicitly the influence of a particular shell with specified occupation can be investigated.

Using Eq. (4) to calculate a configurational average of the cluster scattering path operator $\tau_J(\varepsilon)$ for the disordered case ($\alpha_1=0$), one obtains again an effective (site-diagonal) scattering path operator corresponding to the site at the origin. It should be noted that—considering only a first shell of neighbors—for this average a total of 288 configurations needs to be calculated. This quantity, which shall be termed $\tau_C^{ECM}(\varepsilon)$ reflects now a non-self-consistent averaging including the first-neighbor shell and can be compared with the corresponding (self-consistent) effective scattering path operator $\tau_c^{CPA}(\varepsilon)$ as defined within the single-site KKR-CPA. Table I shows the relative differences of these two quantities at the Fermi energy for the three alloys $Cu_{15}Pt_{85}$, $Cu_{50}Pt_{50}$, and $Cu_{71}Pt_{29}$. The notation used for the irreducible components of the scattering path operator is that of Staunton *et al.*[5] It is indeed amazing to find out from Table I how little these differences are for the "large" diagonal components, carrying practically all the weight in the evaluation of the corresponding partial angular momentum dependent DOS's. The only large difference occurs for the off-diagonal component. Table I illustrates in actual numbers that at the Fermi energy in these three systems obviously fluctuation terms for the CPA condition play only a very minor role, i.e., that the single-site KKR-CPA is indeed a very good approximation for the electronic structure of substitutionally disordered alloys. All physical quantities of substitutionally disordered systems related to the one-particle Green's function, which do not explicitly depend on local neighborhoods, can therefore be expected to be in good agreement with the corresponding experimental data.

Figure 8 finally shows that the calculated values of the single-site KKR-CPA, which served as reference for the present study of short-range-order effects, compare reasonably well with existing experimental values of the linear coefficient of the specific heat. In particular, considering that no electron-phonon enhancement is included to the theoretical values, the linear coefficient of the specific heat is quite accurately described as a function of concentration for noble-metal-rich binary alloys.

IV. CONCLUSION

The present paper presented an extensive study of short-range-order effects for Cu_xPt_{1-x}. It is found that there are certain energy regimes where the local environment has a notable influence on the electronic structure of the investigated substitutionally disordered alloys. It is also found that the single-site KKR-CPA is indeed a very good approximation to describe the effective medium.

ACKNOWLEDGMENTS

The authors are grateful to Dr. P. Marksteiner for many very useful discussions. One of us (P.W.) wants to acknowledge a grant by the Austrian Ministry of Science (under Grant No. G.Z.49.554/3-24/87).

[1]A. Gonis and J. W. Garland, Phys. Rev. B **16**, 2424 (1977).
[2]A. Gonis and A. J. Freeman, Phys. Rev. B **29**, 4277 (1984).
[3]A. Gonis, W. H. Butler, and G. M. Stocks, Phys. Rev. Lett. **50**, 1482 (1983).
[4]A. Gonis, G. M. Stocks, W. H. Butler, and H. Winter, Phys. Rev. B **29**, 555 (1984).
[5]J. Staunton, B. L. Gyorffy, and P. Weinberger, J. Phys. F **10**, 2665 (1980).
[6]P. Weinberger, R. Dirl, A. M. Boring, A. Gonis, and A. J. Freeman, Phys. Rev. B **37**, 1383 (1988).
[7]See, for example, G. M. Stocks and H. Winter, in *The Electronic Structure of Complex Systems, Vol. 113 of NATO ASI Series B,* edited by W. M. Temmerman and P. Phariseau (Plenum, New York, 1984).
[8]R. Dirl, R. Haase, P. Herzig, P. Weinberger, and S. L. Altmann, Phys. Rev. B **32**, 788 (1985).
[9]J. Banhart, H. Ebert, J. Voitländer, and P. Weinberger, Solid State Commun. **65**, 693 (1988).

[10]H. Ebert, P. Weinberger, and J., Voitländer, Phys. Rev. B **31**, 7566 (1985).
[11]J. Banhart, P. Weinberger, and J. Voitländer, J. Phys. Condens. Matter (to be published).
[12]W. H. Fehlner and S. H. Vosko, Can. J. Phys. **54**, 2159 (1976).
[13]F. Duscastelle and F. Gautier, J. Phys. F **11**, 2039 (1976).
[14]A. Bieber, F. Gautier, G. Treglia, and F. Ducastelle, Solid State Commun. **39**, 149 (1981).
[15]A. Gonis, X. G. Zhang, A. J. Freeman, P. Turchi, G. M. Stocks, and D. M. Nicholson, Phys. Rev. B **36**, 4630 (1987).
[16]P. Turchi, G. M. Stocks, W. H. Butler, D. M. Nicholson, and A. Gonis, Phys. Rev. B **37**, 5982 (1988).
[17]P. Weinberger, J. Phys. F **12**, 2171 (1983).
[18]H. Eckardt, L. Fritsche, and J. Noffke, J. Phys. F **14**, 97 (1984).
[19]M. Dixon, F. E. Hoare, and T. H. Holden, Proc. R. Soc. London **90**, 253 (1967).
[20]D. L. Martin, Phys. Rev. B **8**, 5357 (1973).